Phase stability and pressure-induced structural transitions at zero temperature in $ZnSiO_3$ and Zn_2SiO_4

Phase stability and pressure-induced structural transitions at zero temperature in ZnSiO$_3$ and Zn$_2$SiO$_4$

S Zh Karazhanov[1,2,3,5]**, P Ravindran**[1]**, P Vajeeston**[1]**,
A G Ulyashin**[2,6] **and H Fjellvåg**[1] **and B G Svensson**[4]

[1] Centre for Material Science and Nanotechnology, Department of Chemistry,
University of Oslo, PO Box 1033 Blindern, N-0315 Oslo, Norway

[2] Institute for Energy Technology, PO Box 40, N-2027 Kjeller, Norway

[3] Physical-Technical Institute, 2B Mavlyanov Street, Tashkent 700084, Uzbekistan

[4] Department of Physics, University of Oslo, PO Box 1048 Blindern, N-0316 Oslo, Norway

E-mail: smagul.karazhanov@ife.no

Abstract
Using density functional total energy calculations the structural phase stability and
pressure-induced structural transition in different polymorphs of ZnSiO$_3$ and Zn$_2$SiO$_4$ have
been studied. Among the considered monoclinic phase with space groups ($P2_1/c$) and ($C2/c$),
rhombohedral ($R\bar{3}$) and orthorhombic ($Pbca$) modifications the monoclinic phase ($P2_1/c$) of
ZnSiO$_3$ is found to be the most stable one. At high pressure monoclinic ZnSiO$_3$ ($C2/c$) can
co-exist with orthorhombic ($Pbca$) modification. Differences in equilibrium volume and total
energy of these two polymorphs are very small, which indicates that it is relatively easier to
transform between these two phases by temperature, pressure or chemical composition. It can
also explain the experimentally established result of metastability of the orthorhombic phase
under all conditions. The following sequence of pressure-induced structural phase transitions is
found for ZnSiO$_3$ polymorphs: monoclinic ($P2_1/c$) $\rightarrow$ monoclinic ($C2/c$) $\rightarrow$ rhombohedral
($R\bar{3}$). Among the rhombohedral ($R\bar{3}$), tetragonal ($I\bar{4}2d$), orthorhombic ($Pbca$), orthorhombic
($Imma$), cubic ($Fd\bar{3}m$) and orthorhombic ($Pbnm$) modifications of Zn$_2$SiO$_4$, the rhombohedral
phase is found to be the ground state. For this chemical composition of zinc silicate the
following sequence of structural phase transitions is found: rhombohedral ($R\bar{3}$) $\rightarrow$ tetragonal
($I\bar{4}2d$) $\rightarrow$ orthorhombic ($Pbca$) $\rightarrow$ orthorhombic ($Imma$) $\rightarrow$ cubic ($Fd\bar{3}m$) $\rightarrow$ orthorhombic
($Pbnm$). Based on the analogy of crystal structures of magnesium and zinc silicates and using
the lattice and positional parameters of Mg$_2$SiO$_4$ as input, structural properties of spinel
Zn$_2$SiO$_4$ have also been studied.

1. Introduction

Studies of the interface between semiconductors and transparent conducting oxides (TCO) present great interest for optoelectronic device technology. During fabrication of device structures based on contact semiconductor/TCO a mutual diffusion of the atoms from semiconductor to TCO and vice versa can take place at the interface. At high concentrations

of the diffused atoms structural phase transformations can occur, which can result in the formation of new compounds at the interface. Such compounds often possess a wide bandgap and form a band offset with the semiconductor and TCO. From this point of view, a knowledge of structural properties, electronic structure and optical properties of the compounds formed at the interface is important in using them in optoelectronic devices. Further, the crystal structure of compounds formed at the interface will be different from that of the bulk materials due to the interfacial effect and stress in the lattice. So, the structural phase stability studies

---

[5] Author to whom any correspondence should be addressed.
[6] Present address: SINTEF, Materials and Chemistry, PO Box 124 Blindern, N-0314 Oslo, Norway.

of such compounds with pressure present interest from both
fundamental and technologically points of view. It can help to
reveal how the interface influences the operation of a particular
device and to provide the information required to control the
properties of the interface layer.

　　ZnO and Si are the compounds extensively used in modern
semiconductor electronics. The electronegativity of Si and Zn
are 1.90 and 1.65, respectively, which are close to each other.
The atomic sizes of these elements are also comparable to each
other, i.e. 0.117 nm for Si and 0.133 nm for Zn. These data
indicate that the diffusion of Si into ZnO can be favorable. As
a result, at the interface in the heterostructures of Si/ZnO and
SiO_2/ZnO the Si-and Zn-related oxides can be formed, which
will affect the device performance. Polymorphs of $ZnSiO_3$
and Zn_2SiO_4 can be such interfacial oxide layers formed in
between Si/ZnO and SiO_2/ZnO [1, 2] due to the solid state
reaction. These compounds are of particular technological
interest for thin film Si solar cells [3–6], devices where ZnO
is deposited on silicate glass as a TCO buffer layer [7], light-
emitting diodes [8], ZnO nanowires and nanotips grown on
Si and Si on sapphire [9], ZnO particles embedded in sol–gel
silica [1], nanostructures, etc [10–16]. The monoclinic $ZnSiO_3$
nanocrystals have been formed as a result of rapid thermal
annealing of SiO_2 with metallic Zn nanocrystals [17]. Also by
transmission electron microscopy (TEM) with focused electron
beam irradiation, $ZnSiO_3$ nanoparticles have been found in an
SiO_2 layer located in between the ZnO thin film and the Si
substrate [18]. Moreover, from x-ray diffraction, TEM and
selected-area electron diffraction studies it has been found that
orthorhombic $ZnSiO_3$ can be formed at the interface of the
ZnO/Si heterostructure after annealing at 900 °C resulting from
the inter-diffusion between ZnO and Si [19].

　　Crystal structure and structural phase transitions of
$ZnSiO_3$ and Zn_2SiO_4 have been studied experimentally in the
past by many authors (see, e.g., [20–25]) at high temperatures
in the range 700–1500 °C and pressures 0–17 GPa. $ZnSiO_3$
in the monoclinic phase with space group (SG) $C2/c$ is
generally not found to be stable at atmospheric pressure and
it can be obtained as a result of the reaction of willemite
Zn_2SiO_4 with quartz at about 3 GPa and subsequent transition
to ilmenite at 10–12 GPa [20–25] or 15 GPa [26]. However,
it is reported in [21] that $ZnSiO_3$ with SG $C2/c$ also
exists at room temperature and ambient conditions. Upon
increasing the pressure, this phase can undergo the following
sequence of displacive phase transitions from $C2/c$ to a high
pressure phase with SG $P2_1/c(-m_1)$ at 1.92 GPa, which
can also be transformed to another high pressure phase with
SG $C2/c$ ($-m_2$) at 4.9 GPa. However, the differences
in equilibrium volumes between the latter three structural
modifications of $ZnSiO_3$ are too small to consider them as
different polymorphs. Orthorhombic (-o; *Pbca*) $ZnSiO_3$ has
been synthesized at high pressures and temperatures (see,
e.g., [24]) and it is found to be metastable under all conditions.

　　In the polymorphs of $ZnSiO_3$, Zn atoms are coordinated
both octahedrally and tetrahedrally [24] (figure 1). In $ZnSiO_3$-
o the Zn atoms at the octahedral sites have irregular octahedral
coordination to the O atoms. $ZnSiO_3$ of trigonal/rhombohedral
(-r) symmetry with space group $R\bar{3}$ is known by the mineral
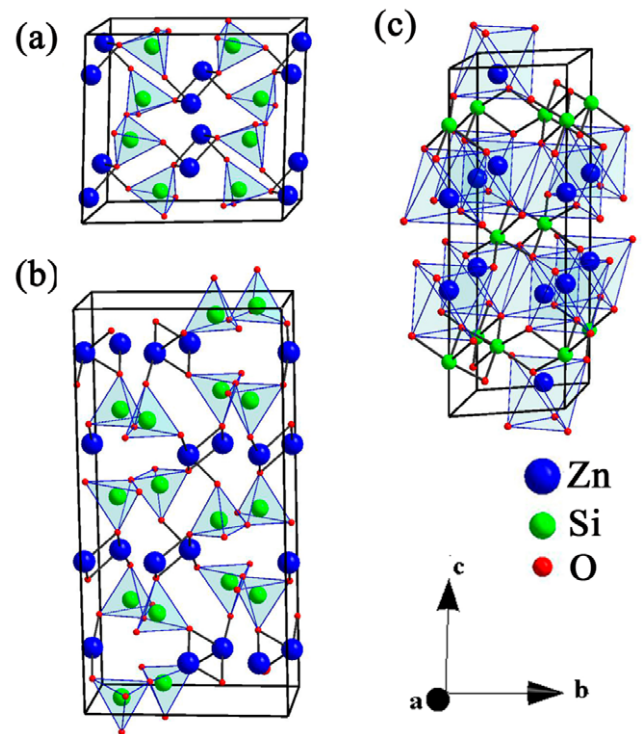
Figure 1. Crystal structures of (a) $ZnSiO_3$-m_2, (b) $ZnSiO_3$-o and
(c) $ZnSiO_3$-r.

name ilmenite. $ZnSiO_3$-r consists of a slightly distorted
hexagonal close-packing array of O atoms with Zn and Si
atoms in the interstitials. Structural properties of these
compounds have been analyzed in more detail in [20, 23, 27].
However, phase stability of different modifications of $ZnSiO_3$
at low temperatures has not been discussed in detail yet.
According to [26] a structural transition from $ZnSiO_3$-m_2 to
-r occurs at 15 GPa at 1000 °C.

　　The Zn_2SiO_4 reported in [28] has been formed as a result
of annealing the ZnO–SiO_x system. Willemite Zn_2SiO_4 has
been formed as a result of the reaction of ZnO with SiO_2 [29],
which has led to a decrease of concentration of the O vacancies
and Zn interstitials. Zn_2SiO_4 has been used to synthesize the
Si-doped ZnO nanobelts [30].

　　Phase transformations of Zn_2SiO_4 have been stud-
ied [31, 24, 27] up to pressures ⩽17 GPa and temperatures
800–1500 °C. The following sequence of structural trans-
formations has been found [27] between five polymorphs of
Zn_2SiO_4: rhombohedral (r) → tetragonal (t) → monoclinic
(m) → orthorhombic (o_1) → orthorhombic (o_2) →
orthorhombic (o_3). Here the o_1, o_2 and o_3 modifications of
the orthorhombic Zn_2SiO_4 denote those with SG symmetry
Pbca, Imma and *Pbnm*, respectively. Owing to the preference
of Zn for tetrahedral rather than octahedral coordination
by oxygen at low pressures, the Zn_2SiO_4 crystallizes into
the phenacite structure with Zn atoms located in distorted
octahedral coordination [14, 26, 22, 23]. In Zn_2SiO_4-t the
oxygen atoms join together with Si and Zn so that each of
the oxygens at the SiO_4 tetrahedra is bonded to Zn atoms,
thus forming an integrated part of a Zn–O–Si network (see
figure 2). The O atoms are located approximately in the
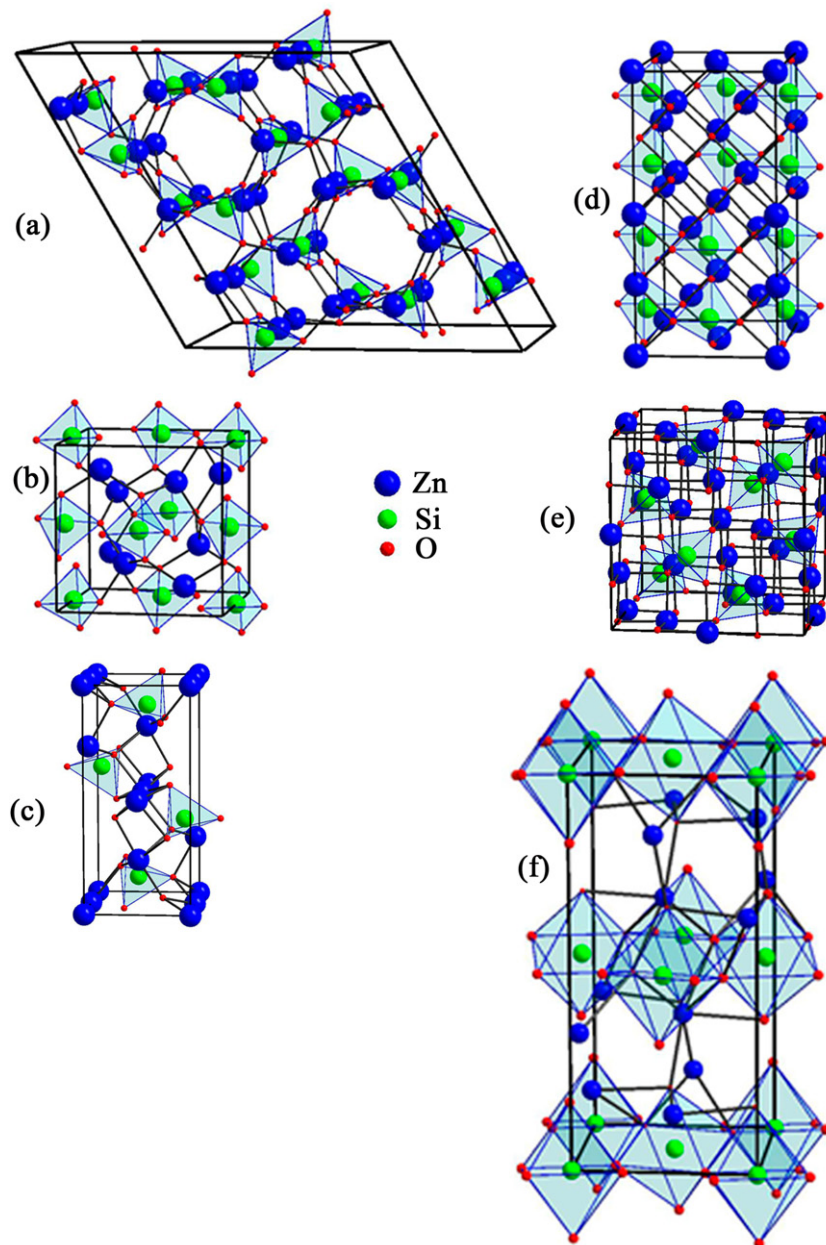
Figure 2. Crystal structures of (a) Zn_2SiO_4-r, (b) Zn_2SiO_4-t, (c) Zn_2SiO_4-o_1, (d) Zn_2SiO_4-o_2, (e) Zn_2SiO_4-c and (f) Zn_2SiO_4-o_3.

body-centered cubic arrangement in Zn_2SiO_4-t, while both the Zn and Si atoms are in tetrahedral coordination to the O atoms. In rhombohedral Zn_2SiO_4 the Zn and Si atoms are also tetrahedrally coordinated to O atoms, where the Zn atoms occupy two crystallographically different sites, but the environments around these sites differ only slightly. Although there is no information about the spinel structure of Zn_2SiO_4, a similar type of compound Mg_2SiO_4 possesses it. The spinels are cubic (-c). They are a class of minerals with the O ions forming a face-centered lattice where Zn cations are octahedrally coordinated and Si atoms are tetrahedrally coordinated.

The above-mentioned experimental results on the existence of different polymorphs of zinc silicates, the possibility of their formation at the interface between ZnO–Si and ZnO–

SiO_2 and the possibility of phase transitions between the polymorphs creates the necessity to study structural properties, electronic structure and optical properties, as well as the interface between the silicates and semiconductors. The study on the electronic structure and optical properties of the intermixed zinc silicates has been performed in [32], which are found to be insensitive to crystal structure modifications and crystallographic directions. Still many questions have been left open. Some of them are the systematic study of bandgap variation in between the zinc silicates and ZnO(Si) and the ways of controlling them, which would be important to know for the influence of the interface layer on current transport. The other one is doping of the silicates by shallow level impurities and H, which allows one to classify the silicates as semiconductors or insulators. However, first of

all it is interesting to know which of the polymorphs of the zinc silicates is the most stable one, whether structural phase transitions can take place at low temperatures and pressures as well and what is the difference between equilibrium volumes of the polymorphs. In the present paper we intend to study these questions for ZnSiO$_3$-o, -m_1, -m_2 and -r as well as for Zn$_2$SiO$_4$-t, -r, -m, -o_1, -o_2, -o_3 and -c.

2. Methods

The computations have been performed using the density functional theory (DFT) within the local density approximation (LDA). Structural relaxations and calculation of total energies have been performed with the projector-augmented-wave method (PAW) [33, 34] as implemented in the Vienna *ab initio* simulation package (VASP) [35] using the Ceperley–Alder data [36] for the correlation energy in the parameterization by Perdew–Zunger [37]. The Zn-3d and -4s, O -2s and -2p and Si-3s and -3p have been considered as the valence electrons. The self-consistent calculations were performed using a $4 \times 4 \times 4$ mesh of special **k**-points. Test calculations showed that a plane-wave cutoff energy of 500 eV is sufficient to describe structural properties of zinc silicates reliably. The convergence was achieved when the forces acting on the atoms were <10 meV Å^{-1} and the total energy difference between two consecutive iterations was $<10^{-6}$ eV.

The crystal structures of different modifications of ZnSiO$_3$ and Zn$_2$SiO$_4$ are presented in figures 1 and 2, respectively. Experimentally determined lattice parameters and positional parameters [38, 21] have been used as input. All configurations were fully relaxed using the conjugate gradient method. Here it should be noted that there is some similarity between the structural phase transitions and crystal structures of ZnSiO$_3$ and MgSiO$_3$ [20, 23–25]. The latter compound is well studied and is a very important material to explore in the mineralogy of the Earth's deep mantle. So, MgSiO$_3$ can be used as a model system in the structural studies of ZnSiO$_3$. In the present paper this similarity shall be used. Due to a lack of experimental data for positional and lattice parameters of ZnSiO$_3$-r and Zn$_2$SiO$_4$-c we have used those for MgSiO$_3$-r and Mg$_2$SiO$_4$-c, respectively, as input for the structural optimization for these two phases.

3. Results

3.1. ZnSiO$_3$

Structural optimization has been performed for all the considered structural modifications by the following procedure: first, atomic positions have been relaxed by the force minimization method, keeping the volume and shape of the crystal fixed. Using the relaxed atomic positions as input, the crystal volume and shape have been relaxed using stress minimization freezing out atomic positions. Then these optimized parameters have been used as input to relax atomic positions, cell volume and shape altogether. Crystal structure information obtained in this way was used as input for calculation of the total energy (E_{tot}) as a function of the cell volume (V). The
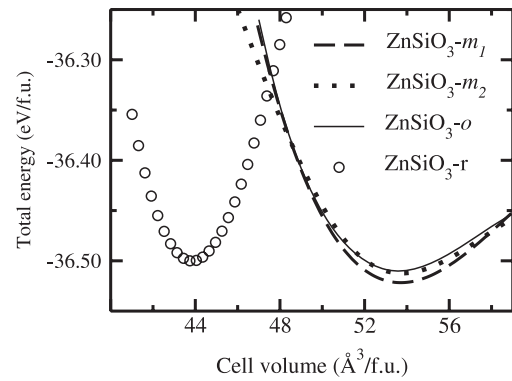
Figure 3. Total energy vs volume curves for ZnSiO$_3$-m_1, -m_2, -o and -r.

minima ($E_{\text{tot}}^{\min}$) of the dependence $E_{\text{tot}}(V)$ are taken as the equilibrium volume. Positional and lattice parameters derived from the DFT calculations for the equilibrium lattices are given in table 1 together with experimentally determined values. Analysis of table 1 shows deviation of the calculated equilibrium volumes from the corresponding experimentally determined values by 2.3% for ZnSiO$_3$-o, 3.3% for ZnSiO$_3$-m_1 and 2.4% for ZnSiO$_3$-m_2. The calculated positional parameters from the structural optimization are found to be overall in good agreement with experimental data. Symmetry of the optimized lattices was checked and found that it is the same as that of the experimentally determined one used as an input for the structural optimization.

Dependence of the total energy on volume has been analyzed for ZnSiO$_3$ (figure 3). The $E_{\text{tot}}(V)$ for ZnSiO$_3$-o is 2.3 meV higher in energy than ZnSiO$_3$-m_2 at their total energy minimum. The magnitude of $E_{\text{tot}}^{\min}$ for ZnSiO$_3$-m_1 is found to be lower than that of ZnSiO$_3$-m_2 by about 10 meV. Consequently, m_2 is the most stable phase. $E_{\text{tot}}^{\min}$ for ZnSiO$_3$-r is found to be about 10 meV higher than that of ZnSiO$_3$-o, which indicates that ZnSiO$_3$-r is the least stable among the considered phases. Since the difference in $E_{\text{tot}}(V)$ between ZnSiO$_3$-o, ZnSiO$_3$-m_1 and -m_2 is not large, a small fluctuation of temperature and pressure can be sufficient to cause the phase transformation between these phases. This result could explain why metastability is observed experimentally for ZnSiO$_3$-o at almost all conditions [24].

Upon compression the volume dependence of E_{tot} for ZnSiO$_3$-m_1 intersects with that for -m_2, -r and -o (figure 3), which indicates the possibility of a phase transition between these modifications. The present calculations suggest that upon compression the following sequence of structural phase transitions can take place (figure 4): one from ZnSiO$_3$-m_1 to ZnSiO$_3$-m_2 and the other from ZnSiO$_3$-m_2 to ZnSiO$_3$-r at pressures of 6.8 and 8.5 GPa, respectively, with corresponding volume shrinkage at the phase transition point 1.1 and 5.24 Å^3/f.u. The calculated transition pressure of 6.8 GPa for the transition ZnSiO$_3$-m_1 $\rightarrow$ ZnSiO$_3$-m_2 somewhat agrees with that of 4.9 GPa obtained from experimental high pressure measurements [21]. The calculated transition pressure for the ZnSiO$_3$-m_1 $\rightarrow$ ZnSiO$_3$-r phase transition is 11.0 GPa and this agrees well with the experimental observation of a

Table 1. Unit cell dimensions and volumes, positional parameters, bulk modulus (B_0), as well as the derivative of bulk modulus (B_0') for $ZnSiO_3$, -*o*, -m_1, -m_2, -m_3, -m_4, -r_1 and -r_2 derived from the density functional total energy calculations at the total energy minimum. Values given in parentheses refer to experimental data [38]. The unit cell volumes are presented per formula unit in Å^3.

Compound	Unit cell (Å)	Atom	Site	X	Y	Z	B_0 (GPa)	B_0'
$ZnSiO_3$-*o*	$a = 17.4224(18.2040)^a$	Zn1	8c	0.1253 (0.1255)	0.3557 (0.3559)	0.4007 (0.4039)	235.8	4.58
$Pbca$	$b = 8.7544(9.0870)^a$	Zn2	8c	0.3760 (0.3761)	0.5140 (0.5092)	0.3949 (0.4005)		
	$c = 5.0881(5.2780)^a$	Si1	8c	0.2742 (0.2741)	0.3373 (0.3363)	0.0852 (0.0867)		
	$V = 53.32(54.57)^a$	Si2	8c	0.4717 (0.4730)	0.1677 (0.1656)	0.2872 (0.2839)		
		O1	8c	0.1840 (0.1853)	0.3318 (0.3346)	0.0831 (0.0820)		
		O2	8c	0.3108 (0.3115)	0.4995 (0.4966)	0.1045 (0.1040)		
		O3	8c	0.3032 (0.3039)	0.2503 (0.2521)	0.3368 (0.3400)		
		O4	8c	0.5624 (0.5621)	0.3355 (0.3389)	0.7863 (0.7800)		
		O5	8c	0.4301 (0.4327)	0.4811 (0.4853)	0.6999 (0.7040)		
		O6	8c	0.4473 (0.4488)	0.2049 (0.2100)	0.5805 (0.5710)		
$ZnSiO_3$-m_1	$a = 9.6543(9.5781)^b$	Zn1	4e	0.2494 (0.2508)	0.6465 (0.6509)	0.2332 (0.2247)	66.5	7.15
$P2_1/c$	$b = 9.0667(8.8905)^b$	Zn2	4e	0.2530 (0.2551)	0.0129 (0.0034)	0.2312 (0.2211)		
	$c = 5.2653(5.1798)^b$	Si1	4e	0.0507 (0.0468)	0.3370 (0.3403)	0.2906 (0.2924)		
	$V = 53.69(51.99)^b$	Si2	4e	0.5583 (0.5568)	0.8332 (0.8338)	0.2500 (0.2397)		
	$\beta = 111.26(109.443)^b$	O1	4e	0.8693 (0.8691)	0.3323 (0.3386)	0.1652 (0.1800)		
		O2	4e	0.3764 (0.3779)	0.8362 (0.8367)	0.1309 (0.1300)		
		O3	4e	0.1231 (0.1169)	0.5000 (0.5033)	0.3537 (0.3365)		
		O4	4e	0.6382 (0.6341)	0.9845 (0.9828)	0.3906 (0.3895)		
		O5	4e	0.1119 (0.1090)	0.2529 (0.2662)	0.5850 (0.5982)		
		O6	4e	0.6079 (0.6078)	0.7051 (0.6965)	0.4893 (0.4702)		
$ZnSiO_3$-m_2	$a = 9.3173(9.787)^a$	Zn1	4e	0.5000 (0.5000)	0.3921 (0.3919)	0.2500 (0.2500)	47.4	4.2
$C2/c$	$b = 9.8180(9.161)^a$	Zn2	4e	0.5000 (0.0000)	0.7289 (0.2361)	0.2500 (0.2500)	$(72.0)^b$	$(7.0)^b$
	$c = 5.0898(5.296)^a$	Si1	8f	0.3060 (0.3016)	0.0837 (0.0849)	0.2646 (0.2668)	(101.0)	
	$V = 53.92(55.26)^a$	O1	8f	0.1238 (0.1241)	0.0833 (0.0868)	0.1427 (0.1473)		
	$\beta = 111.80(111.42)^a$	O2	8f	0.3839 (0.3787)	0.2390 (0.2393)	0.3783 (0.3719)		
		O3	8f	0.3583 (0.3533)	0.0321 (0.0238)	0.0184 (0.0273)		
$ZnSiO_3$-*r*	$a = 4.8115(4.7469)^c$	Zn	6c	0.0000 (0.0000)	0.0000 (0.0000)	0.3692 (0.3599)	177.89	5.5
$R\bar{3}$	$c = 13.9974(13.754)^c$	Si	6c	0.0000 (0.0000)	0.0000 (0.0000)	0.1607 (0.1556)	$(216.0)^{c,d}$	
	$V = 46.77(44.73)^c$	O	18f	0.9911 (0.9645)	0.3736 (0.3200)	0.4286 (0.4896)		

^a From [38]. ^b From [21]. ^c From [23]. ^d From [23, 25].
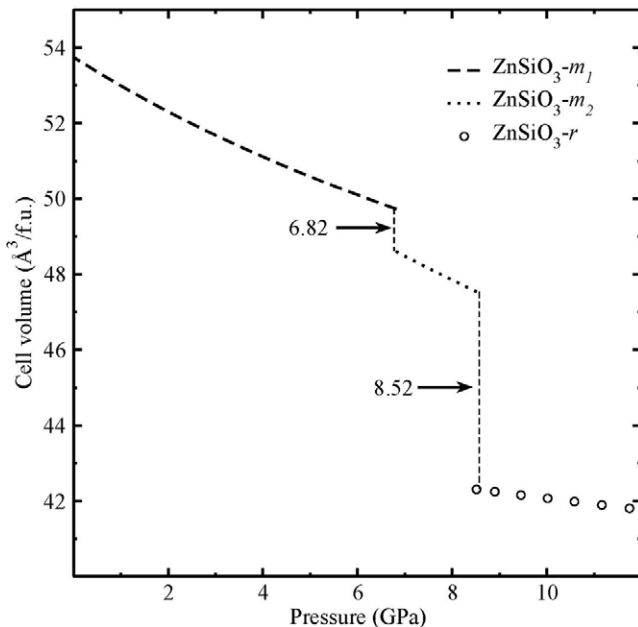
**Figure 4.** Calculated cell volume versus pressure for $ZnSiO_3$-m_1, -m_2 and -*r*.

pressure-induced phase transition from $ZnSiO_3$-*m* to -*r* at 10–12 GPa [20–24] and smaller than 15 GPa [26]. Furthermore, our studies of the pressure dependence of the volume for

$ZnSiO_3$-*r* (figure 5) is found to be in good agreement with recent experimental data from [25].

Bulk modulus (B_0) is the parameter characterizing compressibility of a solid. Among the considered polymorphs of $ZnSiO_3$, the calculated B_0 values vary in the range from 47.4 GPa for $ZnSiO_3$-m_2 to 235.8 GPa for $ZnSiO_3$-*o* (table 1). These analyses show that $ZnSiO_3$-*o* is the hardest phase among the considered polymorphs. The pressure derivative of the bulk modulus (B_0') for some of the silicates is surprisingly large. It equals 4.58 for $ZnSiO_3$-*o*, 7.15 for $ZnSiO_3$-m_1 and 5.5 for $ZnSiO_3$-*r*. We have cross-checked the calculated bulk modulus and its pressure derivative with two independent fitting programs as well as with different equation-of-state models and arrived at the same results.

3.2. Zn_2SiO_4

From the structural optimization the equilibrium structural parameters for different polymorphs of Zn_2SiO_4 have been calculated and presented in table 2. Analysis of table 2 shows that the calculated equilibrium volumes differ from the experimentally determined values by <1.4% for Zn_2SiO_4-o_2, 3.2% for Zn_2SiO_4-*t* and 3.4% for Zn_2SiO_4-*r*. For Zn_2SiO_4-*m* the calculated equilibrium volume is considerable smaller by 8.6% from the experimentally determined one. The discrepancy between the calculated and experimental
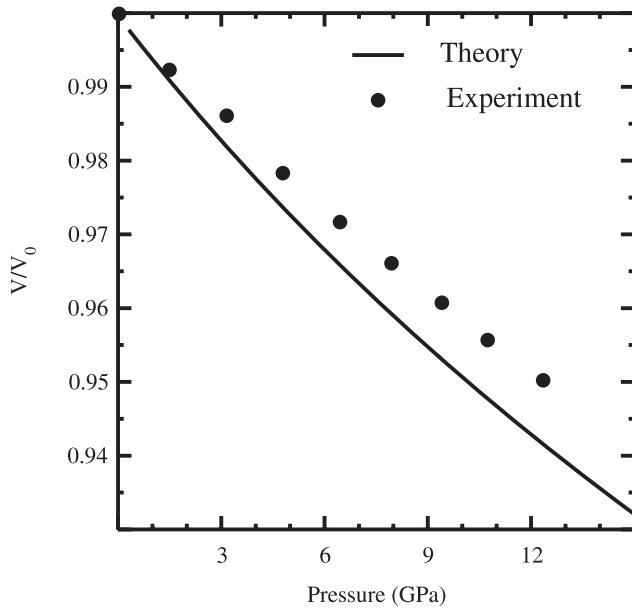
Figure 5. Pressure dependence of the cell volume for ZnSiO$_3$-*r* along with the available experimental data from [25].

Figure 6. Total energy versus volume for Zn$_2$SiO$_4$-*r*, -*t*, -*o$_1$*, -*o$_2$*, -*c*, -*o$_3$* and -*m*.

Figure 7. Calculated cell volume versus pressure for Zn$_2$SiO$_4$-*r*, -*t*, -*o$_1$*, -*o$_2$*, -*c* and -*o$_3$*.

equilibrium volume for different polymorphs may be related to the difference in stoichiometry of the experimentally studied phases and temperature effects, and also uncertainty in some of the lattice and positional parameters. For example, the lattice parameters for Zn$_2$SiO$_4$-*m* and Zn$_2$SiO$_4$-*o$_1$* in [27] correspond to non-stoichiometric crystals with the atomic ratio of Zn:Si = 1.7 and 1.9, respectively, whereas in our calculations the atomic ratio was always Zn:Si = 2. Overall the calculated positional parameters agree well with experimental data given in table 2. We have checked the symmetry of the lattices after structural relaxation and found that their symmetry remain the same as that of the experimentally determined one for all considered polymorphs.

Dependence of the total energy with volume for Zn$_2$SiO$_4$-*r*, -*t*, -*o$_1$*, -*o$_2$*, -*c* and -*o$_3$* are displayed in figure 6. Among these polymorphs, Zn$_2$SiO$_4$-*r* possesses the largest equilibrium volume and smallest total energy at the minimum. Zn$_2$SiO$_4$-*c* possesses the smallest equilibrium volume, but Zn$_2$SiO$_4$-*m* has the largest total energy at E_{tot}^{min} among the considered phases. Consequently, according to our calculations Zn$_2$SiO$_4$-*r* is the most stable phase while Zn$_2$SiO$_4$-*m* is the least stable phase. In addition to the largest total energy, the dependence $E_{tot}(V)$ for Zn$_2$SiO$_4$-*m* is crossed by that of Zn$_2$SiO$_4$-*o$_1$* at its minimum. Consequently, even if Zn$_2$SiO$_4$-*m* has been formed, it can be transformed into Zn$_2$SiO$_4$-*o$_1$*, without pressing or heating.

Analysis of figure 6 shows that the total energy variation with volume for Zn$_2$SiO$_4$-*r* intersects with Zn$_2$SiO$_4$-*t* at high pressure. At more volume compression, $E_{tot}(V)$ for other polymorphs also intersect in the following sequence: Zn$_2$SiO$_4$-*t* with -*o$_1$*, -*o$_1$* with -*o$_2$*, -*o$_2$* with -*c* and -*c* with -*o$_3$*. This result indicates the possibility of pressure-induced phase transition, which is demonstrated in figure 7. The phase transition from Zn$_2$SiO$_4$-*r* to Zn$_2$SiO$_4$-*t* occurs at 0.8 GPa with volume shrinkage 7.3 Å^3/f.u., whereas Zn$_2$SiO$_4$-*t* to Zn$_2$SiO$_4$-*o$_1$* takes place at 15.0 GPa with
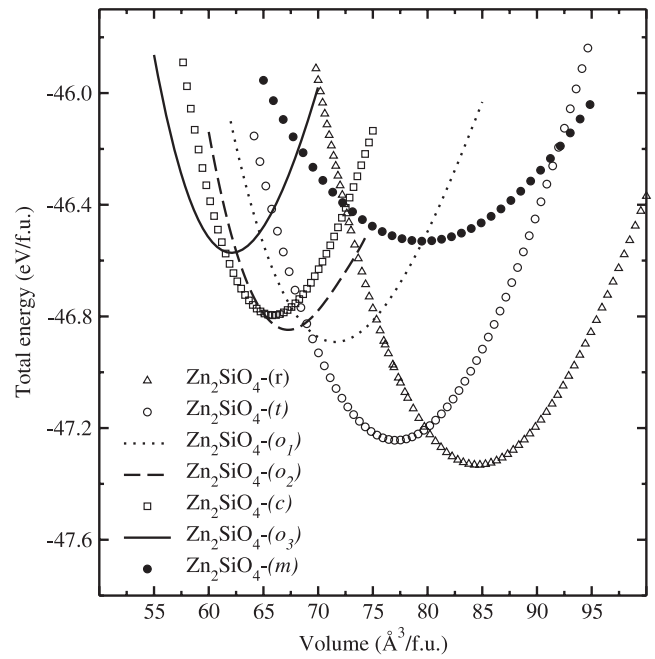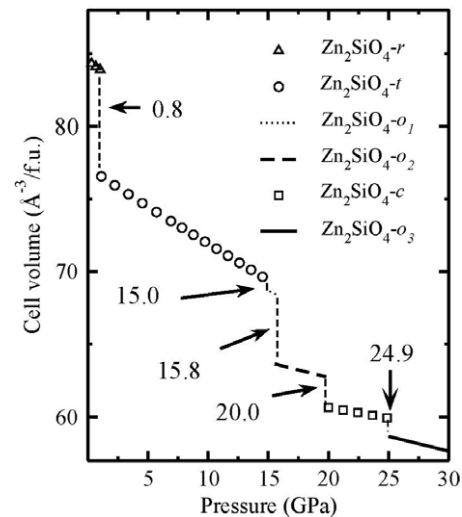
very small volume shrinkage 0.8 Å^3/f.u. Zn$_2$SiO$_4$-*o$_1$* can exist at small pressure range and upon compression it can be transformed into Zn$_2$SiO$_4$-*o$_2$*. The volume variation at the transition Zn$_2$SiO$_4$-*o$_1$* to -*o$_2$* occurring at 15.8 GPa is ~4.7 Å^3/f.u. Upon compression Zn$_2$SiO$_4$-*o$_2$* can transform into Zn$_2$SiO$_4$-*c* at 20.0 GPa (figure 7) with volume shrinkage 2.1 Å^3/f.u. Zn$_2$SiO$_4$-*c* can be transformed to Zn$_2$SiO$_4$-*o$_3$* at 24.9 GPa with small volume variation ~1.3 Å^3/f.u. It should be noted that the present calculations are, strictly speaking, valid only for the stoichiometric compounds at low temperatures. In contrast off-stoichiometry and temperature could stabilize the experimentally identified high pressure

Table 2. Unit cell dimensions, equilibrium volumes, positional parameters, bulk modulus (B_0) and the pressure derivative of bulk modulus (B_0') for Zn_2SiO_4 -*t*, -*r*, -*m*, -o_1, -o_2 and -*c* derived from the density functional total energy calculations at the total energy minimum. Values given in parentheses refer to experimental data [38].

Compound	Unit cell (Å)	Atom	Site	X	Y	Z	B_0 (GPa)	B_0'
Zn_2SiO_4-*r*	$a = 13.8469(13.971)^a$	Zn1	18f	0.1908 (0.1916)	0.2098 (0.2087)	0.5843 (0.5844)	138.8	3.3
$R\bar{3}$	$c = 9.1781(9.3340)^a$	Zn2	18f	0.5264 (0.5579)	0.8818 (0.9655)	0.5841 (0.5815)		
	$V = 84.670(87.66)^a$	Si	18f	0.1951 (0.1963)	0.2127 (0.2118)	0.2499 (0.2510)		
		O1	18f	0.7924 (0.8767)	0.5435 (0.5415)	0.4376 (0.3918)		
		O2	18f	0.1271 (0.1295)	0.2063 (0.3178)	0.3974 (0.3955)		
		O3	18f	0.1083 (0.1100)	0.2127 (0.2175)	0.7507 (0.7496)		
		O4	18f	0.9854 (0.9335)	0.6568 (0.6283)	0.5838 (0.5007)		
Zn_2SiO_4-*t*	$a = 6.9562(7.0069)^b$	Zn	8d	0.1549 (0.1570)	0.2500 (0.2500)	0.1250 (0.1250)	135.8	1.3
$I\bar{4}2d$	$c = 6.3533(6.4637)^b$	Si	4b	0.0000 (0.0000)	0.0000 (0.0000)	0.5000 (0.5000)		
	$V = 76.86(79.38)^b$	O	16e	0.3054 (0.3079)	0.4832 (0.4890)	0.1070 (0.1376)		
Zn_2SiO_4-*m*	$a = 5.3752(5.069)^c$	Zn1	4e	0.3542	0.3811	0.5969	63.0	1.7
$P2_1/n$	$b = 7.8794(10.292)^c$	Zn2	4e	0.4476	0.9915	0.3091		
	$c = 7.5624(6.667)^c$	Si	4e	0.1760	0.7380	0.5414		
	$V = 79.55(87.0)^c$	O1	4e	0.2697	0.9276	0.5053		
	$\beta = 96.55(\sim 90)^c$	O2	4e	0.0135	0.7350	0.7089		
		O3	4e	0.4237	0.6246	0.5874		
		O4	4e	0.0019	0.6468	0.3805		
Zn_2SiO_4-o_1	$a = 4.7231(4.79)^c$	Zn1	4a	0.0000	0.0000	0.0000	157.8	4.3
Pbnm	$b = 10.1975(10.3)^c$	Zn2	4c	0.9850	0.2803	0.2500		
	$c = 5.9430(6.02)^c$	Si	4c	0.4259	0.0960	0.2500		
	$V = 71.56(74.25)^c$	O1	4c	0.7642	0.0936	0.2500		
		O2	4c	0.2164	0.4491	0.2500		
		O3	8d	0.2797	0.1643	0.0335		
Zn_2SiO_4-o_2	$a = 5.8096(5.740)^c$	Zn1	4a	0.0000	0.0000	0.0000	222.0	11.1
Imma	$b = 11.6392(11.504)^c$	Zn2	4e	0.2500	0.7500	0.4683		
	$c = 8.5397(8.395)^c$	Zn3	8g	0.2500	0.1254	0.2500		
	$V = 69.29(69.30)^c$	Si	8h	0.0000	0.1208	0.6164		
		O1	4e	0.0000	0.2500	0.2125		
		O2	4e	0.0000	0.2500	0.7130		
		O3	8h	0.0000	0.4873	0.7579		
		O4	16j	0.2639	0.1229	0.9917		
Zn_2SiO_4-o_3	$a = 4.8891$	Zn	8c	0.9964	0.0553	0.3367	235.8	4.6
Pbca	$b = 4.9980$	Si	4a	0.0000	0.0000	0.0000		
	$c = 10.1666$	O1	8c	0.2012	0.2874	0.0494		
	$V = 62.11$	O2	8c	0.8850	0.9553	0.1588		
Zn_2SiO_4-*c*	$a = 8.0755^c$	Zn	8b	0.5000	0.5000	0.5000	222.2	4.6
$Fd\bar{3}m$	$V = 65.83^c$	Si	32e	0.8750	0.8750	0.8750		
		O	32e	0.2438	0.2438	0.2438		

^{a} From [43]. ^{b} From [31].
^{c} Only lattice parameters of [27] have been used and the positional parameters are from [38] with similar chemical formula and SG, i.e. Ca_2SiO_4 type structure with SG $P2_1/n$ for Zn_2SiO_4-*m*, Ca_2RuO_4 type structure with SG *Pbca* for Zn_2SiO_4-o_3, Mg_2SiO_4 type structure with SG *Imma* for Zn_2SiO_4-o_2 and Mg_2SiO_4 type structure with SG *Pbnm* for Zn_2SiO_4-o_1 have been used for the present computations. Lattice and positional parameters for Zn_2SiO_4-*c* have used Mg_2SiO_4 type structure with SG $Fd\bar{3}m$.

polymorphs such as Zn_2SiO_4-*m*, -o_1, -o_2 and -o_3. In order to clarify the origin of stability of these polymorphs at high pressures and low temperature high pressure experimental measurements on stoichiometric Zn_2SiO_4 at low temperatures are needed.

The calculated bulk modulus for Zn_2SiO_4 polymorphs (table 2) vary in the range from 63.0 GPa for Zn_2SiO_4-*m* to 235.8 GPa for Zn_2SiO_4-o_3. It follows from these analyses that Zn_2SiO_4-o_3 is the hardly compressible phase. The calculated bulk modulus and its pressure derivative for Zn_2SiO_4-*c* is found to be in good agreement (see table 2) with the respective experimentally determined values of 212 GPa and $B_0' = 4$ for Mg_2SiO_4-*c* [39] and the bulk modulus of 216 GPa for Zn_2SiO_4-*c* [23]. This result indicates that the valence and bonding behavior of Zn_2SiO_4 is similar to that of the

geochemically important material Mg_2SiO_4. However, among the considered Zn_2SiO_4 polymorphs, Zn_2SiO_4-*m* is found to be the softest phase.

4. Discussion

One of the important questions is which of the $ZnSiO_3$ and Zn_2SiO_4 polymorphs can be formed at the interface ZnO–Si (SiO_2) and how it depends on growth and device operation conditions. Although some preliminary studies are already available in the literature, there is no systematic study of the point. For example, a crystalline $ZnSiO_3$ is formed [40] upon irradiation of nanocomposite ZnO–SiO_2 films with ultraviolet light because of the photo-induced reaction. From analysis of secondary ion mass spectroscopy inter-diffusion of Zn (Si) into

Si (ZnO) has been reported at the interface between ZnO film and Si substrate [2]. By means of cathodoluminescence and glancing-angle x-ray diffraction the tetragonal modification of Zn_2SiO_4 was proved to be present. Zn_2SiO_4 is also formed at the interface of ZnO/Si heterostructures [5, 2, 41]. It can form a large band offset with Si and ZnO [5], which is assumed to be one of the reasons for the low 8.5% efficiency of crystalline Si–ZnO solar cells [3]. Formation of the rhombohedral modification of Zn_2SiO_4 at the boundary between ZnO particles and the SiO_2 matrix has also been reported [16]. These findings are important and indicate that the idea about the formation of zinc silicates is not far from reality. From the theoretical study of the present paper we found that $ZnSiO_3$-m_1 and Zn_2SiO_4-r are the most stable polymorphs. A systematic experimental study of this point is needed.

The other important point is the pressure at which the stable polymorphs $ZnSiO_3$-m_1 and Zn_2SiO_4-r can be transformed into another one. Analysis of the above theoretical findings corresponding to $T = 0$ K and experimental results corresponding to high temperatures indicates that the transition pressure is very large, which might not be available in $ZnSiO_3$ or Zn_2SiO_4 containing device structures. Consequently, the possibility of phase transitions at ambient pressures (<6.82 GPa for $ZnSiO_3$ and <0.80 GPa for Zn_2SiO_4) can be excluded. This finding has important implications such as, for example, the possibility of lattice expansion/shrinkage. Phase-transition-induced abnormal temperature dependence of electrical conductivities experimentally observed [42] in ZnTe:Cu can also be excluded.

Comparative analysis [32] of electronic structure and optical properties of the $ZnSiO_3$ and Zn_2SiO_4 shows that optical parameters and conduction band electron effective masses of the compounds are almost isotropic and their dependence on crystal structure is negligible. Furthermore, the calculated absorption coefficient, reflectivity, refractive index and extinction coefficients are $<10^3$ cm^{-1}, 0.15, 2.2 and 0.3, respectively, which indicate the possibility of using the zinc silicates as antireflection coatings. Consequently, pressure-induced phase transitions are not expected to cause modulation of optical properties of the ZnO–$ZnSiO_3$ (Zn_2SiO_4)–Si-based device structures.

5. Conclusion

Phase stability and pressure-induced structural transitions between different polymorphs of $ZnSiO_3$ and Zn_2SiO_4 have been studied based on *ab initio* total energy calculations. Among the monoclinic phase with space groups $P2_1/c$ and $C2/c$, rhombohedral ($R\bar{3}$) and orthorhombic ($Pbca$) modifications, the low pressure monoclinic $ZnSiO_3$ phase is found to be the most stable one. Two sequences of structural phase transitions between different modifications of the $ZnSiO_3$ have been found. One sequence is from $ZnSiO_3$ ($P2_1/c$) to $ZnSiO_3$-($C2/c$) and the other one is from $ZnSiO_3$-($C2/c$) to $ZnSiO_3$-$R\bar{3}$. At high pressure monoclinic $ZnSiO_3$ ($C2/c$) can co-exist with orthorhombic ($Pbca$) and equilibrium volume and total energy corresponding

to these two polymorphs are found to be slightly different from each other. This indicates that a small fluctuation in the environment can be sufficient for an orthorhombic to monoclinic transition, which could also explain why the orthorhombic phase is metastable under all conditions. These two polymorphs are found to co-exist in a certain pressure and volume range. According to the present total energy calculations the ilmenite form of $ZnSiO_3$ is found to be the most unstable one at low temperatures and high pressures. Distinct from previous experimental studies at high temperatures, no pressure-induced phase transition has been found into/from this modification. This indicates that the ilmenite phase of $ZnSiO_3$ may be stabilized by the lattice dynamics or oxygen stoichiometry. Among the rhombohedral, tetragonal, orthorhombic, orthorhombic, cubic and orthorhombic modifications of Zn_2SiO_4 the rhombohedral phase is found to be most stable. It can be transformed into the tetragonal phase at high pressures, which upon further compression transformed into a spinel modification. The calculated transition pressures agree with experimental data. Based on analogy with Mg_2SiO_4 orthorhombic Zn_2SiO_4 has been studied. It is found that this polymorph possesses relatively large bulk modulus and, consequently, can be considered as a hardly compressible phase. The presently considered silicates can exist at the interface between ZnO and Si (SiO_2). Although the reported structural transformation between the zinc silicate polymorphs is possible, the transitions occur at high pressures. So, at low pressures, the phase-transition-induced lattice expansion/shrinkage or modulation of the electronic structure and optical properties of the device structures with $ZnSiO_3$ and Zn_2SiO_4 is not expected.

Acknowledgments

References

[1] He H P, Wang Y X and Zou Y M 2003 Photoluminescence property of ZnO–SiO_2 composites synthesized by sol–gel method *J. Phys. D: Appl. Phys.* **36** 2972–5

[2] Xu X *et al* 2003 Formation mechanism of Zn_2SiO_4 crystal and amorphous SiO_2 in ZnO/Si system *J. Phys.: Condens. Matter* **15** L607–13

[3] Kluth O *et al* 1999 Texture etched ZnO: Al coated glass substrates for silicon based thin film solar cells *Thin Solid Films* **351** 247–53

[4] Kobayashi H, Mori H, Ishida T and Nakato Y 1995 Zinc-oxide N–Si junction solar-cells produced by spray-pyrolysis method *J. Appl. Phys.* **77** 1301–7

[5] Meier U and Pettenkofer C 2005 Morphology of the Si–ZnO interface *Appl. Surf. Sci.* **252** 1139–46

[6] Xu X L *et al* 2003 Formation mechanism of Zn_2SiO_4 crystal and amorphous SiO_2 in ZnO/Si system *J. Phys.: Condens. Matter* **15** L607–13

[7] Birkmire R W 2001 Compound polycrystalline solar cells: recent progress and Y2K perspective *Sol. Energy Mater. Sol. Cells* **65** 17–28

[8] Nakanishi Y, Miyake A, Tatsuoka H, Kominami H, Kuwabara H and Hatanaka Y 2005 HRTEM observation of interface states between ZnO epitaxial film and Si(111) substrate *Appl. Surf. Sci.* **244** 359–64

[9] Chen H *et al* 2006 Interface properties of ZnO nanotips grown on Si substrates *J. Electron. Mater.* **35** 1241–5

[10] Amekura H, Kono K, Kishimoto N and Buchal C 2006 Formation of zinc-oxide nanoparticles in SiO_2 by ion implantation combined with thermal oxidation *Nucl. Instrum. Methods Phys. Res.* B **242** 96–9

[11] Amekura H, Sakuma Y, Kono K, Takeda Y, Kishimoto N and Buchal C 2006 Luminescence from ZnO nanoparticles/SiO_2 fabricated by ion implantation and thermal oxidation *Physica* B **376** 760–3

[12] Amekura H *et al* 2006 Zn and ZnO nanoparticles fabricated by ion implantation combined with thermal oxidation, and the defect-free luminescence *Appl. Phys. Lett.* **88** 153119

[13] Amekura H, Umeda N, Yoshitake M, Kono K, Kishimoto N and Buchal C 2006 Formation processes of zinc-oxide nanoparticles by ion implantation combined with thermal oxidation *J. Cryst. Growth* **287** 2–6

[14] Cai Y and Sandhage K H 2005 Aug Zn_2SiO_4-coated microparticles with biologically-controlled 3D shapes *Phys. Status Solidi* a **202** R105–7

[15] Emel'chenko G A *et al* 2005 Opal-ZnO nanocomposites: structure and emission properties *Semiconductors* **39** 1328–32

[16] Ma J G *et al* 2005 Preparation and characterization of ZnO particles embedded in SiO_2 matrix by reactive magnetron sputtering *J. Appl. Phys.* **97** 103509

[17] Yuk J M, Lee J Y, No Y S, Kim T W and Choi W K 2008 Transformation mechanisms from metallic Zn nanocrystals to insulating $ZnSiO_3$ nanocrystals in a SiO_2 matrix due to thermal treatment *Appl. Phys. Lett.* **93** 221910

[18] Shin J W, No Y S, Kim T W and Choi W K 2008 Formation and microstructural properties of locally distributed $ZnSiO_3$ nanoparticles embedded in a SiO_2 layer by using a focused electron beam *J. Nanosci. Nanotechnol.* **8** 5566–70

[19] Yuk J M *et al* 2008 Formation mechanism of $ZnSiO_3$ nanoparticles embedded in an amorphous interfacial layer between a ZnO thin film and an n-Si(001) substrate due to thermal treatment *J. Appl. Phys.* **103** 083520

[20] Akaogi M, Yusa H, Ito E, Yagi T, Suito K and Iiyama J T 1990 The $ZnSiO_3$ clinopyroxene-ilmenite transition—heat-capacity, enthalpy of transition, and phase-equilibria *Phys. Chem. Miner.* **17** 17–23

[21] Arlt T T and Angel R J 2000 Displacive phase transitions in C-centred clinopyroxenes: spodumene, $LiScSi_2O_6$ and $ZnSiO_3$ *Phys. Chem. Miner.* **27** 719–31

[22] Ito E and Matsui Y 1979 High-pressure transformations in silicates, germanates, and titanates with ABO_3 stoichiometry *Phys. Chem. Miner.* **4** 265–73

[23] Leinenweber K, Navrotsky A, McMillan P and Ito E 1989 Transition enthalpies and entropies of high-pressure zinc metasilicates and zinc metagermanates *Phys. Chem. Miner.* **16** 799–808

[24] Morimoto N, Nakajima Y, Syono Y, Akimoto S and Matsui Y 1975 Crystal-structures of pyroxene-type $ZnSiO_3$ and $ZnMgSi_2O_6$ *Acta Crystallogr.* B **31** 1041–9

[25] Sato Y, Ito E and Akimoto S I 1977 Hydrostatic compression of ilmenite phase of $ZnSiO_3$ and $MgGeO_3$ *Phys. Chem. Miner.* **2** 171–6

[26] Ito E and Matsui Y 1975 High-pressure synthesis of $ZnSiO_3$ ilmenite *Phys. Earth Planet. Inter.* **9** 344–52

[27] Syono Y, Akimoto S I and Matsui Y 1971 High pressure transformations in zinc silicates *J. Solid State Chem.* **3** 369–80

[28] Kim H W, Shim S H, Lee J W, Lee C and Jeoung S C 2008 ZnO-sheathed SiO_x nanowires: annealing effect *Opt. Mater.* **30** 1221–4

[29] Chen J K, Tang K L, Tang T P and Chang J T 2008 Effects of zinc oxide and porosity on permittivity of sintered zinc sulfide-silicon dioxide *Japan. J. Appl. Phys.* **47** 5539–44

[30] Cheng B C, Yu X M, Liu H J and Wang Z G 2008 Zn_2SiO_4/ZnO core/shell coaxial heterostructure nanobelts formed by an epitaxial growth *J. Phys. Chem.* C **112** 16312–7

[31] Marumo F and Syono Y 1971 Crystal structure of Zn_2SiO_4-Ii, a high-pressure phase of willemite *Acta Crystallogr.* B **27** 1868

[32] Karazhanov S Z, Ravindran P, Fjellvag H and Svensson B G 2009 Electronic structure and optical properties of $ZnSiO_3$ and Zn_2SiO_4 *J. Appl. Phys.* submitted

[33] Blochl P E 1994 Projector augmented-wave method *Phys. Rev.* B **50** 17953–79

[34] Kresse G and Joubert D 1999 From ultrasoft pseudopotentials to the projector augmented-wave method *Phys. Rev.* B **59** 1758

[35] Kresse G and Furthmüller J 1996 Efficient iterative schemes for *ab initio* total-energy calculations using a plane-wave basis set *Phys. Rev.* B **54** 11169–86

[36] Ceperley D M and Alder B J 1980 *Phys. Rev. Lett.* **45** 566

[37] Perdew J P and Zunger A 1981 *Phys. Rev.* B **23** 5048

[38] *Inorganic Crystal Structure Database* Karlsruhe: Gmelin Institut 2001

[39] Ito E, Akaogi M, Topor L and Navrotsky A 1990 Negative pressure–temperature slopes for reactions forming $MgSiO_3$ perovskite from calorimetry *Science* **249** 1275–8

[40] Taghavinia N, Lee H Y, Makino H and Yao T 2005 Evolution of roughness and photo-crystallization effect in ZnS-SiO_2 nanocomposite films *Nanotechnology* **16** 944–8

[41] Xu X L *et al* 2002 Annealing effect for surface morphology and luminescence of ZnO film on silicon *Chem. Phys. Lett.* **364** 57–63

[42] Zhang J-q *et al* 2002 The structural phase transition and mechanism of abnormal temperature dependence of conductivity in ZnTe:Cu polycrystalline thin films *Thin Solid Films* **414** 113–8

[43] Simonov M A, Sandomirskii P A, Egorovtismenko I K and Belov N V 1977 Crystal-structure of willemite, Zn_2SiO_4 *Dokl. Akad. Nauk SSSR* **237** 581–4